



ARTICLE



The prevalence of adenomyosis in an infertile population: a cross-sectional study



BIOGRAPHY

Dr Hatem Abu Hashim MD, FRCOG, PhD (VUB, Belgium) is a Professor of Obstetrics and Gynecology at Mansoura University, Egypt. His research interests include PCOS, endometriosis and adenomyosis. He is a member of several scientific societies, peer reviews for several international scientific journals and has published several papers in reputed journals.

Hatem Abu Hashim^{1,*}, Solafa Elaraby², Ashraf A. Fouda¹, Mohamed El Rakhawy³

KEY MESSAGE

The observed prevalence of 7.5% for adenomyosis detected *de novo* by two-dimensional transvaginal ultrasound in a population of young infertile women should alert gynaecologists and ultrasonographers to look for the sonographic features of adenomyosis when scanning young infertile women.

ABSTRACT

Research question: Adenomyosis has been reported in a high proportion (24.4%) of infertile women, but this may be over-representative. What is the exact prevalence of adenomyosis in an infertility clinic population?

Design: In this cross-sectional study, 320 infertile women ≤ 41 years of age attending the infertility clinic of a university teaching hospital were screened by two-dimensional transvaginal ultrasound (2D-TVS) to look for the sonographic markers of adenomyosis, with subsequent magnetic resonance imaging (MRI) if suspected. Additionally, the adenomyosis subtype (I–IV) was determined from MRI geography (Kishi classification). Comparisons between women with and without adenomyosis were carried out.

Results: Adenomyosis was found by 2D-TVS in 24 cases (7.5%) and confirmed by MRI in 21 (6.6%). The mean age of the group was 29.2 ± 4.7 years. The most frequently observed sonographic finding (58.3% of cases) was asymmetrical myometrial thickening. The majority of MRI-confirmed cases (85.7%) had diffuse adenomyosis. A significantly higher prevalence was found in women ≥ 40 compared with women < 40 years old (40.0% versus 4.9%, respectively; $P < 0.0001$). Adenomyotic women had significantly higher mean age (32.7 ± 3.0 versus 28.6 ± 4.4 years; $P < 0.00001$), body mass index (31.3 ± 2.7 versus 28.7 ± 3.3 kg/m²; $P < 0.0001$), suffered more dysmenorrhoea (38% versus 17%; $P = 0.02$) and had more ovarian endometriomas (19% versus 6%; $P = 0.03$) than those without adenomyosis.

Conclusion: The observed prevalence of adenomyosis detected *de novo* by 2D-TVS in a population of young infertile women (7.5%) should alert gynaecologists and ultrasonographers to look for the features of adenomyosis when scanning such patients.

¹ Department of Obstetrics and Gynecology, Faculty of Medicine, Mansoura University, Mansoura Dakahlia 35516, Egypt

² Department of Obstetrics and Gynecology, Mansoura General Hospital, Mansoura Dakahlia 35511, Egypt

³ Department of Diagnostic Radiology, Faculty of Medicine, Mansoura University, Mansoura Dakahlia 35516, Egypt

KEYWORDS

Adenomyosis

Infertility

Magnetic resonance imaging

Prevalence

Transvaginal ultrasound

INTRODUCTION

Adenomyosis is a benign gynaecological condition classically described by the presence of ectopic foci of endometrial glands and stroma deeply located in the myometrium with subsequent myometrial inflammation and hypertrophy (Bird and McElin, 1972). Despite having been recognized for over 100 years, adenomyosis still remains a neglected and enigmatic disease, posing a great challenge to both gynaecologists and researchers in the field (Benagiano and Brosens, 2006; Donnez et al., 2018). There is now an accumulating body of evidence concerning the negative impact of adenomyosis on fertility and assisted reproductive technology (ART) outcomes (Rocha et al., 2018; Sharma et al., 2019; Younes and Tulandi, 2017). Disturbances at the endometrial-myometrium interface or uterine junctional zone resulting in disturbed uterine peristalsis and impaired uterotubal transport, as well as implantation failure via altered endometrial function and receptivity, have been reported to explain this negative association. Alternative mechanisms have also been proposed, including uterine contraction mediated by higher prostaglandin production in adenomyotic tissues and excessive free radical release and nitric oxide exposure (Harada et al., 2016; Vlahos et al., 2017).

There is no doubt that histopathological diagnosis following hysterectomy is not a feasible option for infertile women. Fortunately, two-dimensional transvaginal ultrasound (2D-TVS) and magnetic resonance imaging (MRI) have been reported as sufficiently accurate techniques for diagnosis of adenomyosis. The identification of distinct morphological criteria allows a sensitivity and specificity up to 92% and 88% for 2D-TVS and 77% and 89% for MRI, respectively (Andres et al., 2018; Bazot and Daraï, 2018; Bazot et al., 2001; Champaneria et al., 2010; Kepkep et al., 2007; Van den Bosch et al., 2015). Adenomyosis has two main forms, diffuse and focal. In diffuse adenomyosis, ectopic foci of endometrial glands and stroma are evenly scattered in the myometrium, whereas the focal variant is identified by ectopic foci aggregated in a circumscribed nodular manner (Van den Bosch et al., 2015).

A systematic review published in 2012 highlighted the lack of studies evaluating the prevalence of adenomyosis among infertile women (Maheshwari et al., 2012). Since then, it is thought that only one study has been published on this topic. Puente et al. (2016) found adenomyosis in a high proportion (24.4%; $n = 248/1015$) of infertile women by three-dimensional (3D)-TVS. However, the authors admitted that this prevalence might be an overestimate of adenomyosis in the entire infertile population because their study sample included a relatively large proportion of women with repeated ART failures and recurrent miscarriage (36.7%), as well as a number of older women seeking IVF treatment.

In that domain, this study was conducted to determine the prevalence of adenomyosis, initially assessed using 2D-TVS and subsequently confirmed by MRI, in a population of infertile women attending the infertility clinic of a university teaching hospital.

MATERIALS AND METHODS

This was an observational cross-sectional study evaluating infertile women ≤ 41 years of age attending the infertility clinic of the Gynecology Department, Mansoura University Hospitals, Mansoura, Egypt, from October 2013 to June 2017. All women were complaining of infertility, defined as an inability to conceive after 1 year of unprotected intercourse (Zegers-Hochschild et al., 2017). Exclusion criteria were women not complaining of infertility, women ≥ 42 years of age (the clinic is government-funded and only provides treatment for women under the age of 42 years), those complaining of recurrent abortion, those with a previous diagnosis of adenomyosis and those unwilling to participate in the study. The study was approved by the local research ethics committee of the institution (MMREC: Mansoura Medical Research Ethics Committee, code no: MS/195/2013) on 21 May 2013 and all participants gave informed consent before inclusion in the study.

For all women, a detailed clinical history was obtained and a physical examination (general, abdominal and local) was performed prior to the 2D-TVS scan. The pictorial blood loss assessment chart (PBAC) was used to evaluate the amount of menstrual blood loss. Heavy menstrual bleeding (HMB)/menorrhagia was

diagnosed when PBAC score was ≥ 100 (Higham et al., 1990). All investigations previously carried out for infertility such as semen analysis, hysterosalpingogram, hormonal profile, laparoscopy and/or hysteroscopy were reviewed. The information obtained was recorded on a data collection sheet.

The 2D-TVS assessment was performed using a ClearVue 350 ultrasound machine (Philips, Bothell, WA, USA) with a 4–9 MHz transvaginal probe. All scans were done by the same examiner (HAH) during the inter-menstrual phase of the patient's cycle. The uterus was visualized in both longitudinal and transverse planes. The diagnosis of diffuse adenomyosis was made in the presence of one or more morphological sonographic criteria. These criteria were as follows: asymmetrical myometrial thickening, myometrial anechoic cysts, hyperechoic myometrial islands, hyperechoic sub-endometrial linear striations in the myometrium, fan-shaped shadowing and irregular or ill-defined junctional zone. A diagnosis of diffuse adenomyosis was made when one or more of these morphological sonographic criteria were present. Focal adenomyosis was defined as a heterogeneous nodular mass with ill-defined borders (Kepkep et al., 2007; Van den Bosch et al., 2015). Diagnosis of endometriosis was based on a previous laparoscopic report or if an ovarian endometrioma was found during the 2D-TVS scan with the following characteristics: ground glass echogenicity of the cyst fluid (i.e. homogeneous low-level internal echoes) and one to four locules without solid parts (Van Holsbeke et al., 2010).

Subsequently, pelvic MRI examination was carried out in all cases that showed sonographic markers of adenomyosis. MRI was used as a second-line imaging modality for the diagnosis of adenomyosis as well as to differentiate between its subtypes (Bazot and Daraï, 2018). MRI examinations were carried out using a 1.5 T MRI machine (Philips, Ingenia, the Netherlands). Patients were examined in a supine position using a phased-array coil; they were given an anti-peristaltic medication and fasted for 4 h before the examination. The protocol was acquired with a 4 mm thick section and a 1 mm gap, field of view of 25 \times 25 cm and a matrix of 512 \times 512 pixels. MRI sections included sagittal, coronal and axial fast spin-echo T2-

weighted MRI imaging. Sagittal and axial gradient-echo T1-weighted MRI imaging, with and without fat suppression, was also acquired. The following imaging parameters were used for the T2-weighted spin-echo sequence: repetition time ms/echo time ms, 4000/120 (effective); echo train length, 35; and two signals were acquired. T1-weighted spin-echo sequences were performed with 320/4 and one signal was acquired.

The diagnostic criteria for adenomyosis identified on T2-weighted sagittal MRI were: (i) maximal junctional zone thickness (JZ_{max}) ≥ 12 mm (Novellas et al., 2011; Reinhold et al., 1996); (ii) the ratio of the JZ_{max} to the corresponding overall myometrial thickness at the same level of measurement (ratio_{max}) $> 40\%$ (Bazot et al., 2001; Novellas et al., 2011); (iii) high signal intensity myometrial spots (Novellas et al., 2011). Diffuse adenomyosis was diagnosed by at least the association of criteria number (i) and (ii). A low signal intensity mass with ill-defined margins and foci of high signal intensity on T2-weighted images were considered focal adenomyosis (Byun et al., 1999; Novellas et al., 2011). All MRI findings were evaluated by a radiologist experienced in gynaecological MRI (MER) who was blinded to the results from 2D-TVS. Adenomyosis subtype was determined according to the Kishi classification into four subtypes: (i) subtype I or intrinsic, i.e. with direct communication with a thickened junctional zone, but the outer myometrium and serosa are preserved; (ii) subtype II or extrinsic, i.e. originating from the outer uterine layer with intact junctional zone and the muscle layer in between; (iii) subtype III or focal intramural adenomyosis, i.e. solitary lesion with intact junctional zone and serosa and (iv) subtype IV or indeterminate, i.e. did not satisfy any of the aforementioned criteria (Kishi et al., 2012).

Sample size calculation

The sample size of 310 women was established at the study design phase using the following formula:

$$n = \frac{Z^2 P(1-P)}{d^2}$$

where n is the sample size, $Z = 1.96$ for 95% confidence level, P is the expected prevalence in a proportion of 1 and d is the precision ($= 0.05$) (Daniel, 1999). P

was set at 28%, i.e. $P = 0.28$ according to a previous report of a 28% prevalence for adenomyosis (diffuse and focal) by MRI in a control group of young (< 36 years) non-endometriotic women ($n = 19/67$) (Kunz et al., 2005).

Statistical analyses

Data were statistically analysed using SPSS Statistics for Windows, Version 16 (SPSS Inc., Chicago, IL, USA). The normality of data was tested with the Kolmogorov-Smirnov test. Continuous variables were presented as mean \pm SD for parametric data, and median (range) for non-parametric data. Categorical data were described using number and % (n , %). The 95% confidence intervals (CI) for proportions and means were calculated when necessary. Comparisons between adenomyosis positive and negative women were carried out using chi-squared or Fisher's exact tests for categorical variables and Student's *t*-test for those that were continuous. The results were considered significant when the P -value was < 0.05 . Odds ratios (OR) and the mean difference (MD) with 95% CI were calculated for dichotomous and continuous outcomes, respectively.

RESULTS

A total of 355 infertile women were approached to participate in the study; 320 (90.1%) met eligibility criteria and were enrolled. Of these, 264 women (82.5%) had primary infertility and 56 (17.5%) had secondary infertility. The duration of infertility reported ranged from 1 to 15 years with a median of 3 years. Thirty-five women were excluded (FIGURE 1). Among 320 infertile women screened by 2D-TVS, the prevalence of adenomyosis was 7.5% (95% CI 4.6–10.4%; $n = 24/320$). The demographic data of the patient population are shown in TABLE 1. The mean age was 29.2 ± 4.7 years (95% CI 28.7–29.7 years) and the age range was 19–41 years. The characteristics for adenomyosis in the 24 cases identified by 2D-TVS are shown in TABLE 2. Asymmetrical myometrial thickening was observed most frequently (58.3%; 95% CI 38.6–78.0%). Of note, none of the 24 cases had been previously diagnosed with adenomyosis. The diagnosis was subsequently confirmed by MRI in 21 cases. Two cases with suspected focal adenomyosis by 2D-TVS were found to be fibroids on MRI and a case with ill-defined junctional zone by 2D-TVS was found to have a thin

junctional zone by MRI. Therefore, the prevalence of adenomyosis by MRI was 6.6% (95% CI 3.9–9.3%). The MRI characteristics of adenomyosis are shown in TABLE 2. The majority of cases showed diffuse adenomyosis with the $JZ_{max} \geq 12$ mm and ratio_{max} $> 40\%$ (85.7%; 95% CI, 70.7–100.7%) (subtype I Kishi), while focal intramural adenomyosis with an intact thin junctional zone and serosal coat (subtype III Kishi) was less common (14.3%; 95% CI –0.7 to 29.3). No cases of extrinsic (subtype II Kishi) or indeterminate (subtype IV Kishi) adenomyosis were detected by MRI in this study.

The prevalence of MRI-confirmed adenomyosis was significantly higher in women ≥ 40 years compared with women < 40 years [40.0% (6/15) versus 4.9% ($n = 15/305$); OR 12.9; 95% CI 4.1–40.9; $P < 0.0001$]. Of note, the cut-off of 40 years was chosen for comparison in light of previous reports which showed the vast majority (80%) of adenomyosis occurs in women above this age (Bergeron et al., 2006; Harada et al., 2016; Pontis et al., 2016). The prevalence of MRI-confirmed adenomyosis within different age subgroups was: < 30 years = 2/151 (1.3%), 30–33 years = 2/76 (2.6%), 34–37 years = 9/69 (13.0%) and 38–41 years = 8/24 (33.3%), respectively. As shown in TABLE 3, analysis by the chi-squared test for trend revealed a significant association of adenomyosis with female age (chi-squared for linear trend = 31.83; $P < 0.0000001$). The prevalence of adenomyosis was 6.4% ($n = 17/264$) in women with primary infertility and 7.1% ($n = 4/56$) in women with secondary infertility without significant difference (OR 0.9; 95% CI 0.3–2.8; $P = 0.85$).

In this study, MRI-confirmed adenomyotic women had significantly higher mean age (32.7 ± 3.0 versus 28.6 ± 4.4 years; MD 4.0; 95% CI 2.6–5.4 years; $P < 0.00001$), body mass index (BMI) (31.3 ± 2.7 versus 28.7 ± 3.3 ; MD 2.6; 95% CI 1.4–3.8; $P < 0.0001$) and suffered more dysmenorrhoea (38% versus 17%; OR 3.0; 95% CI 1.2–7.6; $P = 0.02$) than those without adenomyosis. However, no between-group differences in gravidity, parity, HMB, deep dyspareunia and other variables were found (TABLE 1). There was no significant difference in the observed rates of associated fibroids between groups; however, adenomyotic patients were more likely to have ovarian

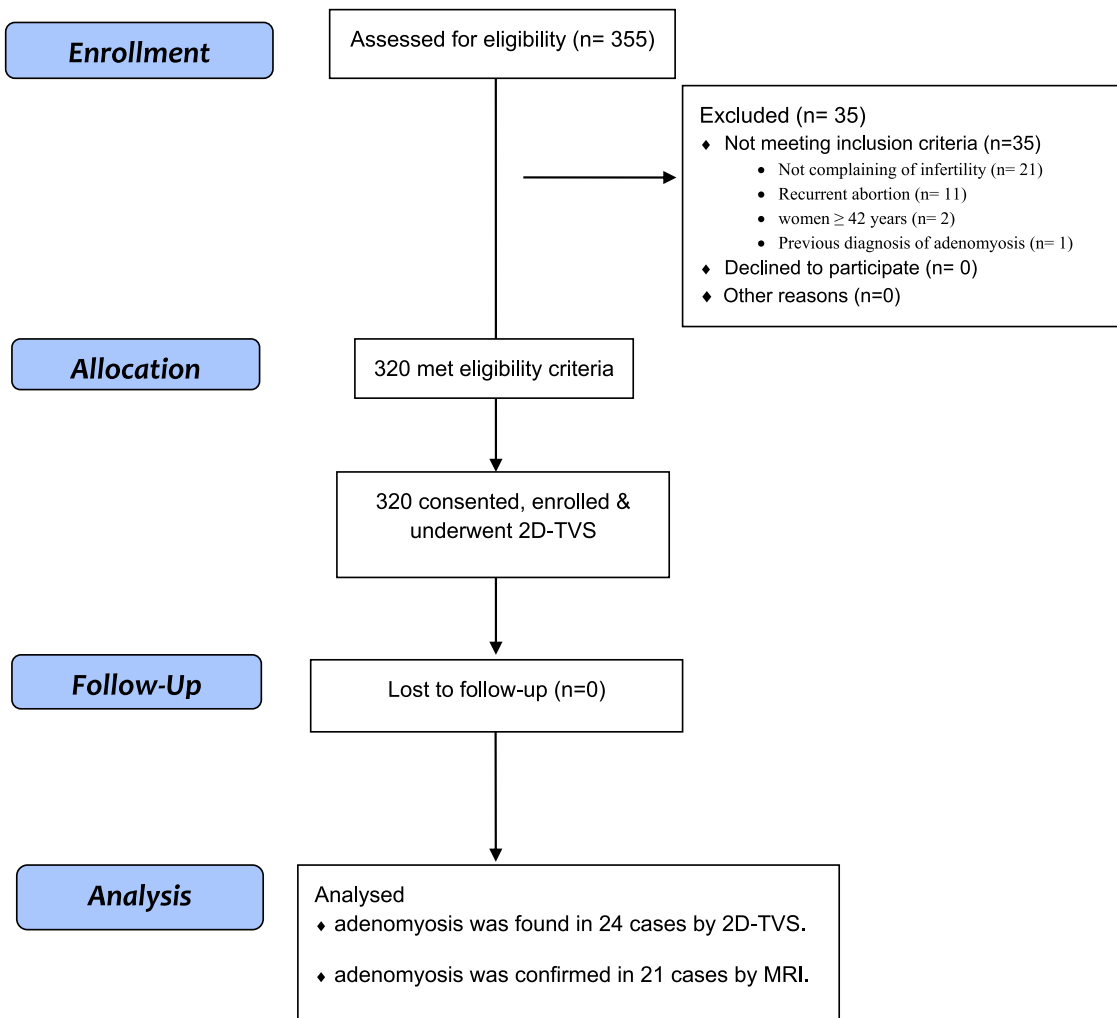


FIGURE 1 Study flow diagram. 2D-TVS = two-dimensional transvaginal ultrasound; MRI = magnetic resonance imaging.

endometriomas [19% (4/21) versus 6% ($n = 18/299$); OR 3.7; 95% CI 1.1–12.1; $P = 0.03$] (TABLE 1). Selections from the MRI scans of adenomyotic patients are shown in FIGURES 2 to 4.

DISCUSSION

As revealed by 2D-TVS, the prevalence of adenomyosis in this study was 7.5%. Among the MRI-confirmed 21 adenomyotic women, the majority (85.7%) showed diffuse adenomyosis (subtype I Kishi). Adenomyotic women had significantly higher mean age, BMI, suffered more dysmenorrhoea and had a higher incidence of ovarian endometriomas than those without adenomyosis. The lower prevalence of adenomyosis (7.5%) detected in this study compared with that of *Punete et al. (2016)* (24.4%) is likely to be explained by the lower mean age of patients (29.2 ± 4.7 years) versus 38.3 ± 4.1 and 37.2

± 4.7 years in positive and negative adenomyotic cases, respectively. Other explanations for the higher prevalence of adenomyosis observed by *Puente et al. (2016)* may be the selection biases in 36.7% of their cases as previously mentioned (see Introduction), as well as the use of 3D-TVS, which has the advantage of evaluating the junctional zone better than 2D-TVS (*Exacoustos et al., 2011; Rasmussen et al., 2019*). The finding of a higher prevalence of adenomyosis in women ≥ 40 years agrees with *Puente et al. (2016)*. Furthermore, analysis for linear trend across age subgroups revealed a significant association of adenomyosis with female age, which is pronounced in women aged > 33 years (TABLE 3). This observation corresponds with previous findings by *Kunz et al. (2007)*, who reported a marked increase in the junctional zone thickness indicative of adenomyosis after the age of 34 years in 227 women

evaluated by MRI. This could be related to the ageing progress of the uterus with more prolonged endogenous oestrogen exposure (*Garcia and Isaacson, 2011; Kunz et al., 2005, 2007*).

Despite the previously reported increased frequency of adenomyosis in multiparous patients and those with a previous spontaneous abortion (*Garcia and Isaacson, 2011; Parazzini et al., 1997; Templeman et al., 2008*), no difference was found between the prevalence of adenomyosis in primary and secondary infertility cases. This may be explained by the small number of cases suffering from secondary infertility (17.5%). The finding of no differences in parity status was also reported by *Puente et al. (2016)*.

In this study, asymmetrical myometrial thickening was the most frequently observed sign of adenomyosis on 2D-TVS (58.3%) (TABLE 2). Similar findings were

TABLE 1 PATIENT CHARACTERISTICS AND COMPARISON BETWEEN CASES WITH AND WITHOUT MRI-CONFIRMED ADENOMYOSIS

Variable	Total cohort ^a (n = 320)	MRI-confirmed adenomyosis (n = 21)	No adenomyosis (n = 299)	OR (95% CI)	P-value
Age (years) ^b	29.2 ± 4.7	32.7 ± 3.0	28.6 ± 4.4	4 (2.6, 5.4) ^c	<0.00001 ^d
BMI (kg/m ²)	27.8 ± 2.3	31.3 ± 2.7	28.7 ± 3.3	2.6 (1.4, 3.8) ^c	<0.0001 ^d
Age at menarche (years)	12.6 ± 1.0	12.9 ± 0.7	12.6 ± 1.0	0.3 (-0.04, 0.6) ^c	0.09
Menstrual cycle					
Regular	243 (75.9)	18 (85.7)	225 (75.3)	2 (0.6, 6.9)	0.29
Irregular	77 (24.1)	3 (14.2)	74 (24.7)	0.5 (0.1, 1.8)	
HMB (menorrhagia): (PBAC ≥100)	67 (20.9)	4 (19)	63 (21.1)	0.9 (0.3, 2.7)	0.83
Dysmenorrhea	59 (18.4)	8 (38)	51 (17.1)	3 (1.2, 7.6)	0.02 ^d
Gravidity					
0	265 (82.8)	17 (81.0)	248 (82.9)	0.9 (0.3, 2.7)	0.82
1	38 (11.9)	2 (9.5)	36 (12.0)	0.8 (0.2, 3.4)	0.73
>1	17 (5.3)	2 (9.5)	15 (5.0)	2 (0.4, 9.4)	0.38
Parity					
0	284 (88.8)	19 (90.5)	265 (88.6)	1.2 (0.3, 5.5)	0.80
1	35 (10.9)	2 (9.5)	33 (11)	0.8 (0.2, 3.8)	0.83
>1	1 (0.3)	0 (0)	1 (0.3)	4.6 (0.2, 117.0)	0.35
Oral contraceptive use					
Previous user	12 (3.8)	2 (9.5)	10 (3.3)	3.0 (0.6, 14.9)	0.17
Never	308 (96.3)	19 (90.5)	289 (96.7)	0.3 (0.1, 1.6)	
Abortions	26 (8.1)	2 (9.5)	24 (8.0)	1.2 (0.3, 5.5)	0.81
Deep dyspareunia	35 (10.9)	2 (9.5)	33 (11.0)	0.8 (0.2, 3.8)	0.83
Associated fibroids	51 (15.9)	5 (23.8)	46 (15.4)	1.7 (0.6, 4.9)	0.31
Associated ovarian endometrioma	22 (6.9)	4 (19.0)	18 (6.0)	3.7 (1.1, 12.1)	0.03 ^d

All data are expressed as n (%) or mean ± SD.

^a 305 women (95.3%) <40 years and 15 (4.7%) ≥40 years.

^b Range: 19–41, 27–41 and 19–41 years in total cohort, positive and negative cases respectively.

^c Mean difference (95% CI).

^d Significant (P < 0.05).

BMI = body mass index; CI = confidence interval; HMB = heavy menstrual bleeding; OR = odds ratio; PBAC = pictorial blood loss analysis chart.

reported among 53 young nulliparous women with diffuse adenomyosis by 2D-TVS (56.6%) (Pinzauti *et al.*, 2015). The majority of cases in this study were diffuse adenomyosis (85.7%) confirmed by MRI (TABLE 2, FIGURE 2A–D and FIGURE 3A). This finding confirms that intrinsic adenomyosis (subtype I Kishi) is more common than focal intramural adenomyosis (subtype III Kishi) (Kishi *et al.*, 2012). No cases of extrinsic adenomyosis (subtype II Kishi) were found, which could be explained by the current lack of knowledge about the role of TVS in its detection (Bazot and Daraï, 2018). The finding of three cases with isolated focal adenomyoma and an intact thin junctional zone and serosal coat (subtype III Kishi) (TABLE 2, FIGURES 3C and D and FIGURE 4A–D) could support the hypothesis concerning metaplasia for this subtype (Bergeron *et al.*, 2006; García-

Solares *et al.*, 2018; Kishi *et al.*, 2012). Of note, Kishi *et al.* (2012) highlighted that focal adenomyosis occurred more frequently in younger women (mean age 34.3 ± 4.7 years).

In contrast to the findings of Puente *et al.* (2016), this study showed that adenomyotic women had a significantly higher mean age than those without adenomyosis (TABLE 1). This may be related to a longer duration of oestrogen exposure (Garcia and Isaacson, 2011). Increased BMI has been reported as a risk factor for adenomyosis (Templeman *et al.*, 2008). This is consistent with the findings of this study (TABLE 1). Adenomyosis is considered as a cause of abnormal uterine bleeding owing to increased uterine volume, vascularity, abnormal uterine contractions, and increased oestrogen and prostaglandin

production (Abbott, 2017; Munro *et al.*, 2011). Heavy menstrual bleeding was found in 19% of the adenomyotic women in this study (TABLE 1), a similar value to that found by others (18.9%) (Pinzauti *et al.*, 2015). In this study, adenomyotic patients also experienced more dysmenorrhoea (TABLE 1) than women without adenomyosis. Of note, Kissler *et al.* (2008) reported thickening of the junctional zone suggestive of adenomyosis in 87% (26/30) of infertile patients suffering from severe dysmenorrhoea.

A significant association was found between adenomyosis and ovarian endometriomas (FIGURE 4). This is supported by other investigators who reported that adenomyotic patients were more likely to have other markers of severe endometriosis such as ovarian

TABLE 2 2D-TVS AND MRI CHARACTERISTICS OF ADENOMYOSIS

2D-TVS findings	n (%), 95% CI	No. of women
Asymmetric myometrial thickness ^a	14 (58.3, 38.6 to 78.0)	
Cystic anechoic spaces in the myometrium ^a	7 (29.1, 10.9 to 47.3)	
Fan-shaped shadowing ^a	5 (20.8, 4.6 to 37.0)	
Sub-endometrial echogenic linear striations ^a	3 (12.5, -0.7 to 25.7)	
Irregular or ill-defined JZ	2 (8.3, -2.7 to 19.3)	
Intramural mass ?? fibroid ?? focal adenomyosis	5 (20.8, 4.6 to 37.0)	
Number of 2D-TVS criteria per 24 women		
3 criteria		1
2 criteria		10
1 criterion		8
? focal adenomyosis		5
MRI characteristics of adenomyosis		
Maximal JZ thickness (JZ _{max}) ≥12 mm	18 (85.7, 70.7 to 100.7)	
Ratio _{max} (JZ _{max} /myometrial thickness) >40%	18 (85.7, 70.7 to 100.7)	
High signal intensity myometrial spots ^a	10 (47.6, 26.2 to 69.0)	
Focal adenomyosis	3 (14.3, -0.7 to 29.3)	
Number of MRI criteria of adenomyosis per 21 women		
3 criteria		10
2 criteria		8
Focal adenomyosis		3

^a Finding associated with others.

2D-TVS = two-dimensional transvaginal ultrasound; CI = confidence interval; JZ = junctional zone; max = maximal; MRI = magnetic resonance imaging.

endometriomas and deep infiltrating endometriosis (Puente *et al.*, 2016). This finding was also reported in patients with MRI diagnosis of adenomyosis (Chapron *et al.*, 2017; Zacharia *et al.*, 2006). This association necessitates a reconsideration of the contribution of adenomyosis to infertility in this subset of women.

The strength of this study is that a population of young infertile patients without a previous diagnosis of adenomyosis was screened. Adenomyosis was diagnosed by reliable 2D-TVS markers and all scans were performed by a single operator, thereby minimizing

inter-observer variability. Additionally, predefined unique MRI diagnostic criteria were used by an experienced radiologist who was blinded to the results from 2D-TVS. This maximized the accuracy of the diagnosis, especially in women who had an associated leiomyoma and when the sonographic diagnosis was uncertain. Moreover, findings were not only interpreted as diffuse or focal adenomyosis, but also differentiation of the adenomyosis subtype based on MRI geography was carried out. This complementary role of MRI could be attributed to the opportunity to examine

a volume of tissue in multiple slices and spatial relations.

On the other hand, this study has limitations. First, the sample size ($n = 320$) may be regarded as relatively small. However, this sample size was based on an *a priori* power calculation taking into account the findings of a previous study pertinent to this issue (Kunz *et al.*, 2005). The lack of histopathological confirmation for adenomyosis may limit diagnostic accuracy. However, hysterectomy is not a feasible option for infertile women. The lack of 3D-TVS may be regarded

TABLE 3 ANALYSIS FOR LINEAR TREND OF MRI-CONFIRMED ADENOMYOSIS ACROSS AGE SUBGROUPS

Age subgroup (years)	Score ^a	Positive adenomyosis (n = 21)	No adenomyosis (n = 299)	Total (n = 320)	OR
<30	1	2	149	151	1.00
30-33	2	2	74	76	2.01
34-37	3	9	60	69	11.18
38-41	4	8	16	24	37.25

Chi-squared for linear trend (extended Mantel-Haenszel) = 31.83.

P-value (1 degree of freedom) = <0.0000001.

^a A numeric score assigned across the age subgroups starting from number 1 for the subgroup with the lowest prevalence and 4 for the subgroup with the highest prevalence of adenomyosis.

MRI = magnetic resonance imaging; OR = odds ratio.

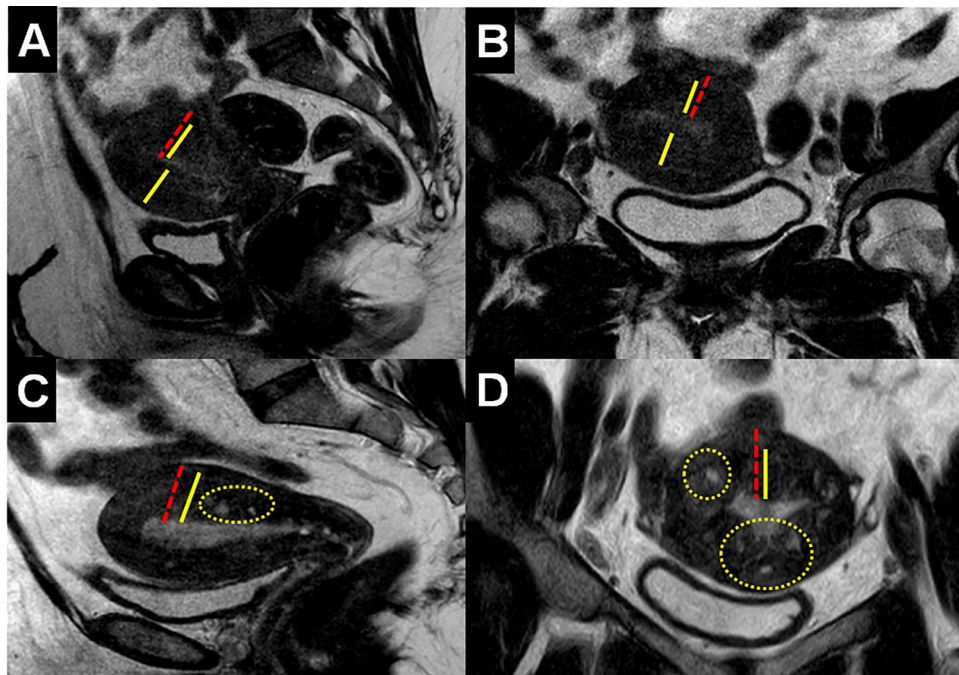


FIGURE 2 MRI showing diffuse adenomyosis. (A and B) Sagittal and coronal T2-weighted MRI sections from a 32-year-old woman showing marked thickening of the junctional zone (yellow lines) in both anterior and posterior uterine walls with preserved outer myometrium and serosa (subtype I Kishi) (Kishi *et al.*, 2012). Posterior wall myometrial thickness is marked by the broken red line. (C and D) Sagittal and coronal T2-weighted MRI sections from a 29-year-old woman showing marked thickening of the junctional zone (yellow line) of the posterior uterine wall with numerous foci of high signal intensity (broken yellow circles) in the posterior myometrium in both sections and in the anterior myometrium in coronal section. The outer myometrium and serosa remain intact (subtype I Kishi) (Kishi *et al.*, 2012). Posterior wall myometrial thickness is marked by the broken red line.

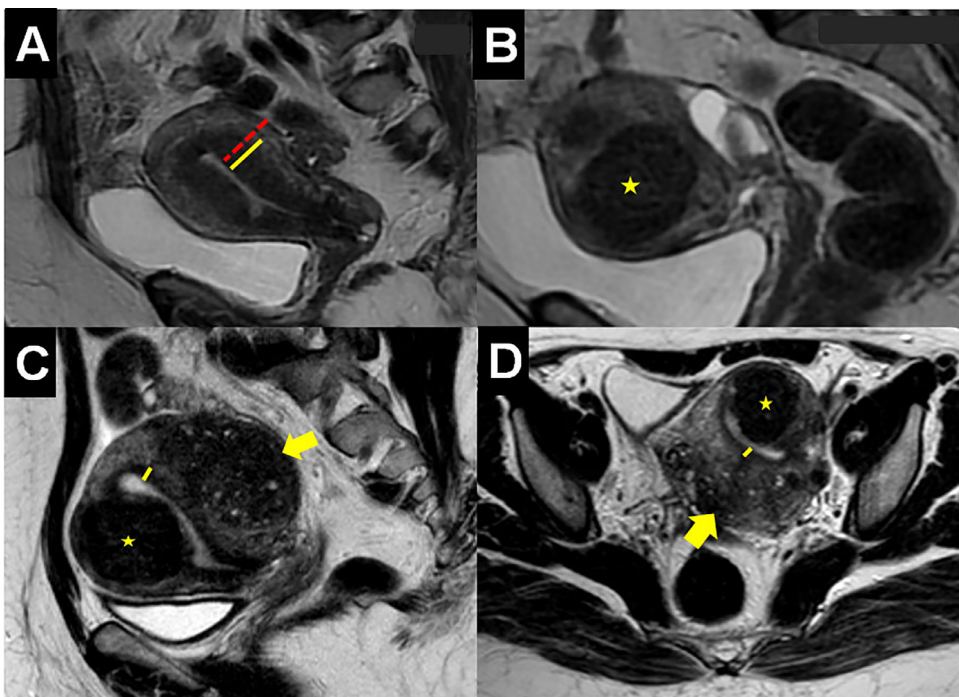


FIGURE 3 MRI showing diffuse and focal adenomyosis with associated fibroids. (A) Sagittal T2-weighted MRI section from a 31-year-old woman showing diffuse adenomyosis with preserved outer myometrium and serosa (subtype I Kishi) (Kishi *et al.*, 2012). The posterior junctional zone is marked by yellow line and posterior wall myometrial thickness is marked by broken red line. (B) Sagittal T2-weighted MRI section (same patient as Figure 3A) with associated intramural fibroid (yellow star) measuring 4.5×4 cm. (C and D) Sagittal and axial T2-weighted MRI sections from a 28-year-old woman showing focal adenomyosis with numerous foci of high signal intensity located in the posterior myometrium (yellow arrow) with associated anterior intramural fibroid 3.5×4.5 cm (yellow star). The junctional zone (yellow line) and serosa are kept intact (subtype III Kishi) (Kishi *et al.*, 2012).

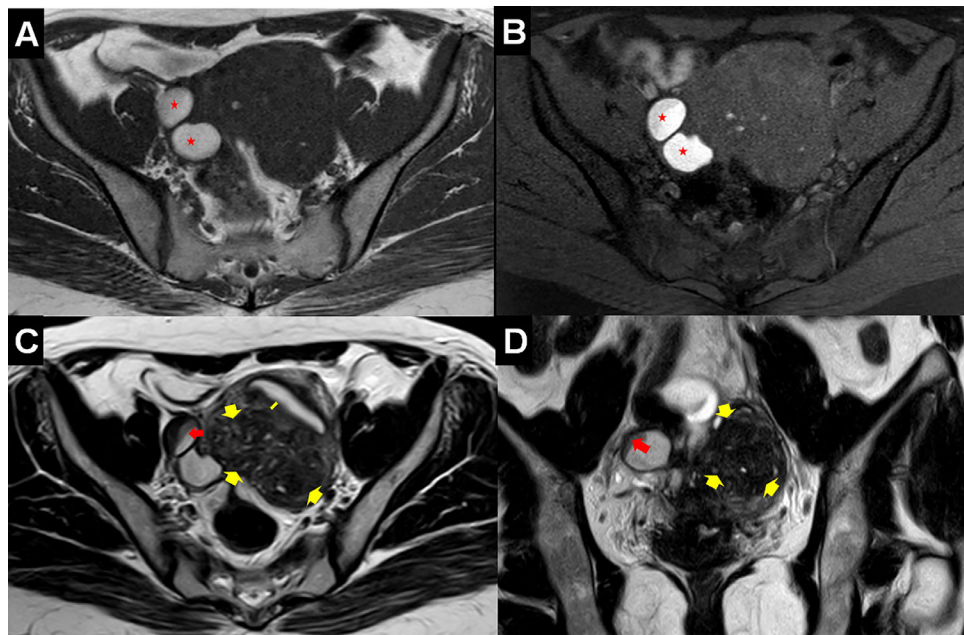


FIGURE 4 MRI showing focal adenomyosis with an associated ovarian endometrioma in a 34-year-old woman. (A) Axial T1-weighted MRI section showing a right bilocular ovarian endometrioma measuring 5 × 4 cm (red stars). (B) Axial T1-weighted MRI section with fat suppression showing very hyperintense blood containing bilocular right ovarian endometrioma (red stars). (C and D) Axial and coronal T2-weighted MRI sections showing localized posterior adenomyosis (subtype III Kishi) (yellow arrows) and right ovarian endometrioma with shading effect (red arrows). The intact junctional zone is marked by the yellow line in the axial section.

as another limitation. Of note, a recent meta-analysis reported no difference in the overall accuracy of 3D-TVS compared with 2D-TVS except in junctional zone assessment (Andres *et al.*, 2018). Optimizing junctional zone details by 3D-TVS could be useful in the diagnosis of adenomyosis (Exacoustos *et al.*, 2011; Rasmussen *et al.*, 2019).

In conclusion, data from this study showed the prevalence of adenomyosis detected *de novo* in a population of young infertile women as measured by 2D-TVS to be 7.5%. It is important for gynaecologists and ultrasonographers to keep this observation in mind during their daily practice by looking for the 2D-TVS diagnostic criteria of adenomyosis when scanning young infertile women. Large-scale studies are needed to generate a body of evidence about the prevalence of adenomyosis in other age groups and to define different populations in the same age range who need assessment (e.g. differences based on race, BMI, comorbidities). Moreover, in light of the recently published consensus by the International Deep Endometriosis Analysis group (Guerriero *et al.*, 2016), we think that future studies assessing the prevalence of adenomyosis in infertile women should consider

these markers (uterine and adnexa mobility tenderness, sliding sign and deep endometriotic nodules in different compartments) as a complementary step after mapping for sonographic markers of adenomyosis and concomitant endometriomas. This may be of added value for an in-depth evaluation of both entities in infertile women.

REFERENCES

- Abbott, J.A. **Adenomyosis and Abnormal Uterine Bleeding (AUB-A)—Pathogenesis, diagnosis, and management**. Best. Pract. Res. Clin. Obstet. Gynaecol. 2017; 40: 68–81
- Andres, M.P., Borrelli, G.M., Ribeiro, J., Baracat, E.C., Abrão, M.S., Kho, R.M. **Transvaginal Ultrasound for the Diagnosis of Adenomyosis: Systematic Review and Meta-Analysis**. J. Minim. Invasive. Gynecol. 2018; 25: 257–264
- Bazot, M., Cortez, A., Darai, E., Rouger, J., Chopier, J., Antoine, J.M., Uzan, S. **Ultrasonography compared with magnetic resonance imaging for the diagnosis of adenomyosis: correlation with histopathology**. Hum. Reprod. 2001; 16: 2427–2433
- Bazot, M., Daraï, E. **Role of transvaginal sonography and magnetic resonance imaging in the diagnosis of uterine adenomyosis**. Fertil. Steril. 2018; 109: 389–397
- Benagiano, G., Brosens, I. **History of adenomyosis**. Best Pract. Res. Clin. Obstet. Gynaecol. 2006; 20: 449–463
- Bergeron, C., Amant, F., Ferenczy, A. **Pathology and physiopathology of adenomyosis**. Best. Pract. Res. Clin. Obstet. Gynaecol. 2006; 20: 511–521
- Bird, C.C., McElin, T.W., Manalo-Estrella, P. **The elusive adenomyosis of the uterus—revisited**. Am. J. Obstet. Gynecol. 1972; 112: 583–593
- Byun, J.Y., Kim, S.E., Choi, B.G., Ko, G.Y., Jung, S.E., Choi, K.H. **Diffuse and focal adenomyosis: MR imaging findings**. Radiographics 1999; 19: S161–S170
- Champaperia, R., Abedin, P., Daniels, J., Balogun, M., Khan, K.S. **Ultrasound scan and magnetic resonance imaging for the diagnosis of adenomyosis: systematic review comparing**

test accuracy. *Acta Obstet. Gynecol. Scand.* 2010; 89: 1374–1384

Chapron, C., Tosti, C., Marcellin, L., Bourdon, M., Lafay-Pillet, M.C., Millischer, A.E., Streuli, I., Borghese, B., Petraglia, F., Santulli, P. **Relationship between the magnetic resonance imaging appearance of adenomyosis and endometriosis phenotypes.** *Hum. Reprod.* 2017; 32: 1393–1401

Daniel, W.W. 1999 **Biostatistics: a foundation for analysis in the health sciences.** Seventh ed. John Wiley and Sons New York, USA

Donnez, J., Donnez, O., Dolmans, M.M. **Introduction: Uterine adenomyosis, another enigmatic disease of our time.** *Fertil. Steril.* 2018; 109: 369–370

Exacoustos, C., Brienza, L., Di Giovanni, A., Szabolcs, B., Romanini, M.E., Zupi, E., Arduini, D. **Adenomyosis: three-dimensional sonographic findings of the junctional zone and correlation with histology.** *Ultrasound Obstet. Gynecol.* 2011; 37: 471–479

Garcia, L., Isaacs, K. **Adenomyosis: review of the literature.** *J. Minim. Invasive. Gynecol.* 2011; 18: 428–437

García-Solares, J., Donnez, J., Donnez, O., Dolmans, M.M. **Pathogenesis of uterine adenomyosis: invagination or metaplasia?** *Fertil. Steril.* 2018; 109: 371–379

Guerrero, S., Condous, G., van den Bosch, T., Valentín, L., Leone, F.P., Van Schoubroeck, D., Exacoustos, C., Instalé, A.J., Martins, W.P., Abrao, M.S., Hudelist, G., Bazot, M., Alcazar, J.L., Gonçalves, M.O., Pascual, M.A., Ajossa, S., Savelli, L., Dunham, R., Reid, S., Menákaya, U., Bourne, T., Ferrero, S., Leon, M., Bignardi, T., Holland, T., Jurkovic, D., Benacerraf, B., Osuga, Y., Somigliana, E., Timmerman, D. **Systematic approach to sonographic evaluation of the pelvis in women with suspected endometriosis, including terms, definitions and measurements: a consensus opinion from the International Deep Endometriosis Analysis (IDEA) group.** *Ultrasound Obstet. Gynecol.* 2016; 48: 318–332

Harada, T., Khine, Y.M., Kaponis, A., Nikellis, T., Decavalas, G., Taniguchi, F. **The Impact of Adenomyosis on Women's Fertility.** *Obstet. Gynecol. Surv.* 2016; 71: 557–568

Higham, J.M., O'Brien, P.M.S., Shaw, R.W. **Assessment of menstrual blood loss using a pictorial chart.** *Br. J. Obstet. Gynaecol.* 1990; 97: 734–739

Kepkep, K., Tuncay, Y.A., Göynümer, G., Tural, E. **Transvaginal sonography in the diagnosis of adenomyosis: which findings are most accurate?** *Ultrasound Obstet. Gynecol.* 2007; 30: 341–345

Kishi, Y., Suginami, H., Kuramori, R., Yabuta, M., Suginami, R., Taniguchi, F. **Four subtypes of adenomyosis assessed by magnetic resonance imaging and their specification.** *Am. J. Obstet. Gynecol.* 2012; 207: 114

Kissler, S., Zangos, S., Kohl, J., Wiegratz, I., Rody, A., Gätje, R., Vogl, T.J., Kunz, G., Leyendecker, G., Kaufmann, M. **Duration of dysmenorrhoea and extent of adenomyosis visualized by magnetic resonance imaging.** *Eur. J. Obstet. Gynecol. Reprod. Biol.* 2008; 137: 204–209

Kunz, G., Beil, D., Huppert, P., Noe, M., Kissler, S., Leyendecker, G. **Adenomyosis in endometriosis—prevalence and impact on fertility. Evidence from magnetic resonance imaging.** *Hum. Reprod.* 2005; 20: 2309–2316

Kunz, G., Herbertz, M., Beil, D., Huppert, P., Leyendecker, G. **Adenomyosis as a disorder of the early and late human reproductive period.** *Reprod. Biomed. Online* 2007; 15: 681–685

Maheshwari, A., Gurunath, S., Fatima, F., Bhattacharya, S. **Adenomyosis and subfertility: a systematic review of prevalence, diagnosis, treatment and fertility outcomes.** *Hum. Reprod. Update* 2012; 18: 374–392

Munro, M.G., Critchley, H.O., Broder, M.S., Fraser, I.S. **FIGO classification system (PALM-COEIN) for causes of abnormal uterine bleeding in nongravid women of reproductive age.** *Int. J. Gynaecol. Obstet.* 2011; 113: 3–13

Novellas, S., Chassang, M., Delotte, J., Toullalan, O., Chevallier, A., Bouaziz, J., Chevallier, P. **MRI characteristics of the uterine junctional zone: from normal to the diagnosis of adenomyosis.** *Am. J. Roentgenol.* 2011; 196: 1206–1213

Parazzini, F., Vercellini, P., Panazza, S., Chatenoud, L., Oldani, S., Crosignani, P.G. **Risk factors for adenomyosis.** *Hum. Reprod.* 1997; 12: 1275–1279

Pinzauti, S., Lazzari, L., Tosti, C., Centini, G., Orlandini, C., Luisi, S., Zupi, E., Exacoustos, C., Petraglia, F. **Transvaginal sonographic features of diffuse adenomyosis in 18–30-year-old nulligravid women without endometriosis: association with symptoms.** *Ultrasound Obstet. Gynecol.* 2015; 46: 730–736

Pontis, A., D'Alterio, M.N., Pirarba, S., de Angelis, C., Tinelli, R., Angioni, S. **Adenomyosis: a systematic review of medical treatment.** *Gynecol. Endocrinol.* 2016; 32: 696–700

Puente, J.M., Fabris, A., Patel, J., Patel, A., Cerrillo, M., Requena, A., Garcia-Velasco, J.A. **Adenomyosis in infertile women: prevalence and the role of 3D ultrasound as a marker of severity of the disease.** *Reprod. Biol. Endocrinol.* 2016; 14: 60. doi:10.1186/s12958-016-0185-6

Rasmussen, C.K., Hansen, E.S., Ernst, E., Dueholm, M. **Two- and three-dimensional transvaginal ultrasonography for diagnosis of adenomyosis of the inner myometrium.** *Reprod. Biomed. Online* 2019; 38: 750–760

Reinhold, C., McCarthy, S., Bret, P.M., Mehio, A., Atri, M., Zakarian, R., Glaude, Y., Liang, L., Seymour, R.J. **Diffuse adenomyosis: comparison of endovaginal US and MR imaging with histopathologic correlation.** *Radiology* 1996; 199: 151–158

Rocha, T.P., Andres, M.P., Borrelli, G.M., Abrão, M.S. **Fertility-Sparing Treatment of Adenomyosis in Patients With Infertility: A Systematic Review of Current Options.** *Reprod. Sci.* 2018; 25: 480–486

Sharma, S., Bathwal, S., Agarwal, N., Chattopadhyay, R., Saha, I., Chakravarty, B. **Does presence of adenomyosis affect reproductive outcome in IVF cycles? A retrospective analysis of 973 patients.** *Reprod. Biomed. Online* 2019; 38: 14–21

Templeman, C., Marshall, S.F., Ursin, G., Horn-Ross, P.L., Clarke, C.A., Allen, M., Deapen, D., Ziogas, A., Reynolds, P., Cress, R., Anton-Culver, H., West, D., Ross, R.K., Bernstein, L. **Adenomyosis and endometriosis in the California Teachers Study.** *Fertil. Steril.* 2008; 90: 415–424

Van den Bosch, T., Dueholm, M., Leone, F.P., Valentín, L., Rasmussen, C.K., Votino, A., Van Schoubroeck, D., Landolfo, C., Instalé, A.J., Guerrero, S., Exacoustos, C., Gordts, S., Benacerraf, B., D'Hooghe, T., De Moor, B., Brölmann, H., Goldstein, S., Epstein, E., Bourne, T., Timmerman, D. **Terms, definitions and measurements to describe sonographic features of myometrium and uterine masses: a consensus opinion from the Morphological Uterus Sonographic Assessment (MUSA) group.** *Ultrasound Obstet. Gynecol.* 2015; 46: 284–298

Van Holsbeke, C., Van Calster, B., Guerrero, S., Savelli, L., Paladini, D., Lissoni, A.A., Czekierowski, A., Fischerova, D., Zhang, J., Mestdagh, G., Testa, A.C., Bourne, T., Valentín, L., Timmerman, D. **Endometriomas: their ultrasound characteristics.** *Ultrasound Obstet. Gynecol.* 2010; 35: 730–740

Vlahos, N.F., Theodoridis, T.D., Partsinevelos, G.A. **Myomas and Adenomyosis: Impact on Reproductive Outcome.** *Biomed. Res. Int.* 2017; 20175926470. doi:10.1155/2017/5926470

Younes, G., Tulandi, T. **Effects of adenomyosis on in vitro fertilization treatment outcomes: a meta-analysis.** *Fertil. Steril.* 2017; 108: 483–490

Zacharia, T.T., O'Neill, M.J. **Prevalence and distribution of adnexal findings suggesting endometriosis in patients with MR diagnosis of adenomyosis.** *Br. J. Radiol.* 2006; 79: 303–307

Zegers-Hochschild, F., Adamson, G.D., Dyer, S., Racowsky, C., de Mouzon, J., Sokol, R., Rienzi, L., Sunde, A., Schmidt, L., Cooke, I.D., Simpson, J.L., van der Poel, S. **The International Glossary on Infertility and Fertility Care, 2017.** *Hum. Reprod.* 2017; 32: 1786–1801

Received 7 November 2019; received in revised form 10 February 2020; accepted 17 February 2020.